

PHYS 590 Honours Thesis:  
The Acoustic Laser

Ryan Wicks

6 April 2005

## **Abstract**

*The effect of acoustic lasing has been successfully explained and demonstrated. The equations governing this effect have been derived from the fundamental equations of fluid dynamics, and these have been used to numerically model the effect two different ways. The demonstrated directionality of the signals is better than that of conventional emitters/speakers (approximately 40 times better at 1000 Hz). These methods could easily be extended to more complicated systems and geometries, suitable for an engineering design problem.*

---

## Contents

<b>I</b>	<b>Introduction</b>	<b>2</b>
1	Background	2
2	A Survey of Acoustic Lasing	2
<b>II</b>	<b>Theory</b>	<b>2</b>
<b>3</b>	<b>The Non-Linear Wave Equation</b>	<b>3</b>
3.1	Fundamental Equations . . . . .	3
3.2	The Wave Equation . . . . .	3
3.3	The Source Term . . . . .	4
3.4	Method of Solution . . . . .	6
3.5	Form of $\mathbf{v}$ . . . . .	7
4	Green's Function for the Scalar Wave Equation	7
5	Real Emitters	8
<b>III</b>	<b>Models</b>	<b>8</b>
<b>6</b>	<b>Point Model</b>	<b>8</b>
6.1	Timed Speakers and the Green's Function . . . . .	8
6.2	Line Distribution . . . . .	9
6.3	Cylindrical Distribution . . . . .	11
7	Numerical Solutions of the Non-Linear Wave Equations	14
<b>IV</b>	<b>Conclusions</b>	<b>16</b>
<b>V</b>	<b>Appendices</b>	<b>18</b>
A	Derivation of the Non-Linear Wave Equation	18
B	Multi-Dimensional Integrals	20
C	Cylindrical Co-ordinates	21

## Part I

# Introduction

## 1 Background

The purpose of this thesis project was to develop a model for an acoustic laser from the most general equations of fluid dynamics and model it numerically. It was motivated in an earlier Engineering Physics Thesis by Sameer Chandani [Chandani(1998)], assessing the effect for use in hearing aids.

An acoustic laser is a highly directed beam of audible sound produced by a single source <sup>1</sup>, hence the term laser. This effect has been demonstrated, and even marketed (under trade names like HyperSonic<sup>TM</sup> Sound)<sup>2</sup> <sup>3</sup>. It was originally developed for use in Naval sonar systems, as well as for underwater communication, in the form of a *parametric acoustic array* [Westervelt(1960)].

## 2 A Survey of Acoustic Lasing

The term laser is used because this effect is similar to that of a real laser. Aside from emitting a highly directed beam, both systems also possess a gain medium. In the acoustic laser, this gain medium is the region of air directly in front of the emitter/speaker. As a signal travels from the emitter along the gain medium, its amplitude is amplified coherently.

The acoustic laser is one of the problems that falls outside the domain of regular acoustics. Directed beams of sound can be created using large arrays of carefully timed speakers (similar to a phased array radar system [Brookner(1985)]), but creating one from a single emitter is not possible without taking into account non-linear effects.

Consider, for the case of an audible beam, 2 high intensity ultrasound waves of similar frequency (one of them modulated with an audio signal), interfering with each other in air. Where these finite amplitude waves interfere, an audible signal equal to the modulating frequency is created. If the amplitude of the interfering waves is strong enough, non-linear effects allow the signal to exist independent of the original waves, turning the air into an emitter of audible sound. This is called *scattering of sound by sound* [Westervelt(1957), Bellin and Beyer(1957)].

This effect, along with the intensity distribution of real emitters (at high frequencies, the signal tends to be confined to a long and narrow region)(section 5), creates an array of emitters that emit the modulating signal in such a way as to reinforce preferentially in one direction.

---

<sup>1</sup>Many emitters placed close together can also be used. This is called a *parametric acoustic array*.

<sup>2</sup><http://www.holosonics.com/technology.html>

<sup>3</sup><http://www.atcsd.com/pdf/HSSWHTPAPERREV4.pdf>

## Part II

# Theory

### 3 The Non-Linear Wave Equation

In this section, the non-linear wave equation is derived from the fundamental equations of fluid mechanics. An inhomogeneous wave equation is obtained. This equation is simplified and put into a form that can be solved using a Greens function (section 4).

#### 3.1 Fundamental Equations

The four equations that can be used to develop the non-linear wave equation for a perfect gas not subject to body forces (ie. gravity) are as follows [Landau and Lifshitz(2004), Blackstock(2000)]:

$$\frac{\partial \rho}{\partial t} + \nabla \cdot (\rho \mathbf{v}) = 0 \quad (1)$$

$$\frac{\partial \mathbf{v}}{\partial t} + (\mathbf{v} \cdot \nabla) \mathbf{v} + \frac{\nabla p}{\rho} = 0 \quad (2)$$

$$p = p_o \left( \frac{\rho}{\rho_o} \right)^\gamma \quad (3)$$

$$\gamma = \frac{C_p}{C_v} \quad (4)$$

Where  $\rho$  is gas density ( $\rho_o$  is the background density),  $p$  is the pressure ( $p_o$  is the background pressure), and  $\mathbf{v}$  is the gas velocity. These equations (1 - 3) are the continuity (1), momentum (Euler's equation) (2), and state (3) equations (where (4) is the ratio of specific heats). Euler's equation is used instead of the full Navier-Stokes equations because this thesis is primarily concerned with signals propagating in air, which has low viscosity (high Reynold's number)(the Navier-Stokes equations reduce to Euler's equation when viscosity is neglected). The adiabatic equation of state (3) is an excellent approximation for wave motion in air in almost all cases (always for regular acoustic problems)([Hall(1987)]).

#### 3.2 The Wave Equation

The standard wave equation has the form given in equation 5.

$$\frac{\partial^2 \delta}{\partial t^2} - c^2 \nabla^2 \delta = 0 \quad (5)$$

$$\delta = \frac{\rho - \rho_o}{\rho_o} \quad (6)$$

This equation assumes small signal strength. It is in terms of the fractional change in density (equation 6). It can also be re-written in terms of  $p$ ,  $\rho$ ,  $\mathbf{v}$  or  $\Phi$  (where  $\mathbf{v} = -\nabla\Phi$ , the velocity potential). The use of these variables implies that wave motion in a fluid involves longitudinal (compression and rarefaction) waves, rather than transverse ones. It can be solved by separation of variables, is linear in both variables and allows for an infinite set of orthogonal solutions.

This equation cannot be used to fully model acoustic lasing. The superposition of large amplitude signals entails non-linear effects. The non-linear wave equation is derived in Appendix A, including explanations of the simplifications that would lead to equation 5, the linear wave equation. The full non-linear wave equation for a fluid with no viscosity or heat conduction is given in equation 7.

$$\frac{\partial^2 \delta}{\partial t^2} - c^2 \nabla^2 \delta = S(\mathbf{r}, t) \quad (7)$$

$$S(\mathbf{r}, t) = c^2 \frac{\gamma - 1}{2} \nabla^2 \delta^2 + \nabla \delta \cdot (\mathbf{v} \cdot \nabla) \mathbf{v} + (\delta + 1) \nabla \cdot ((\mathbf{v} \cdot \nabla) \mathbf{v}) - \nabla \cdot \left( \frac{\partial \delta}{\partial t} \mathbf{v} \right) - c^2 \frac{(\gamma - 1)(\gamma - 2)}{6} \nabla^2 \delta^3 + \dots \quad (8)$$

Where  $S(\mathbf{r}, t)$  is the source term. All higher order terms come from the binomial expansion of  $p$  (equation 33 in Appendix A) (replace the  $(\dots)$  with the term of interest from equation 33 multiplied by  $\frac{1}{\rho_0}$  and substitute for  $c^2 = \frac{p_0}{\rho_0} \gamma$ ).

### 3.3 The Source Term

Equation 7 has the same form as the linear wave equation (equation 5) with the addition of a higher order source term (equation 8). The choice to binomial expand the equation of state (equation 3) for  $p$  puts equation 7 into the form of an inhomogeneous wave equation, but with the inhomogeneous source term involving an infinite sum. Fortunately, these terms decrease quickly as the order of the term increases.

The fractional change in density  $\delta$  at a point will have the form of a constant ( $C$ ) multiplied by a sinusoid varying in time. For most systems, it is reasonable to expect that  $\delta$ , and  $C$ , will be small, and so higher order terms can be neglected. Deciding where the series must be truncated involves carefully consideration of the conditions leading to an acoustic laser.

By assuming that  $\mathbf{v}$  has a similar dependence on  $C$  as  $\delta$  (which will be shown explicitly later), the source term can be separated into terms of order  $C^2$ ,  $C^3$ , and so on.  $C$  can be estimated for different sound pressure levels (measured in decibels) and the equation of state. The decibel scale is defined in equation 9 [Young and Freedman(1996)].

$$dB = 20 \log_{10} \left( \frac{p_{max}}{p_{ref}} \right) \quad (9)$$

Where  $p_{ref} = 2 \times 10^{-5} Pa$  and  $p_{max}$  is the maximum amplitude of the pressure. Using the equation of state for an adiabatic gas, equation 3 and the definition of the fractional change in density, equation 6, an expression for C can be obtained (equation 10).

$$c = \left( \frac{p_{ref} 10^{\frac{dB}{20}}}{p_o} + p_o \right)^{\frac{1}{\gamma}} - 1 \quad (10)$$

Plotted in figure 1 is C against decibels in air.

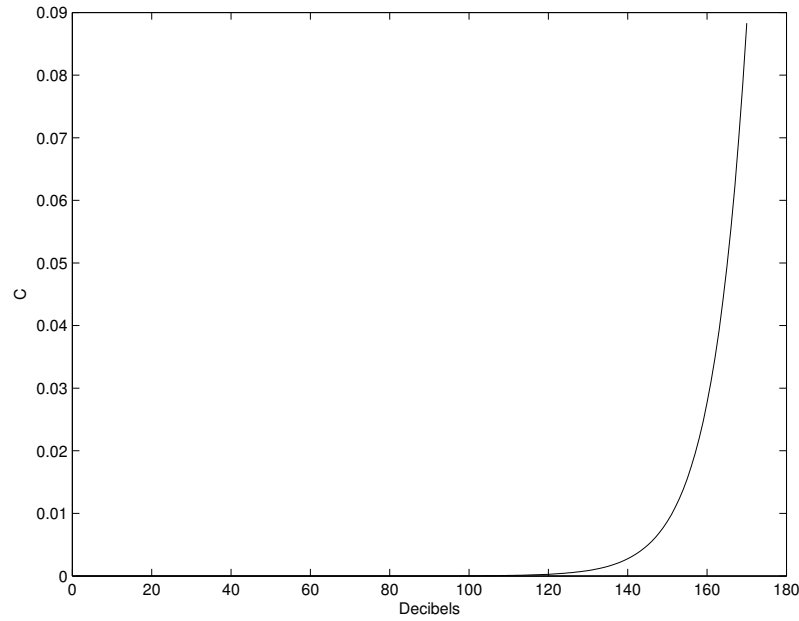


Figure 1: C Against Decibels for Air

C is a small number, even for very large driving fields. Past 170 dB in air, C does become large, but when signals reach this strength, earlier approximations break down and other effects must be taken into account (like cavitation and shock wave effects [Landau and Lifshitz(2004)]). Also, very few speakers couple efficiently enough to air to reach this signal strength ([Blackstock(2000)]). So, it is a good approximation to neglect any terms higher than second order, resulting in the simplified non-linear wave equation, equation 11.

$$S(\mathbf{r}, t) = c^2 \frac{\gamma - 1}{2} \nabla^2 \delta^2 + \nabla \cdot ((\mathbf{v} \cdot \nabla) \mathbf{v}) - \nabla \cdot \left( \frac{\partial \delta}{\partial t} \mathbf{v} \right) \quad (11)$$

Further simplifications can be made by expanding out the  $(\mathbf{v} \cdot \nabla) \mathbf{v}$  term using the identity in equation 12 [Jackson(1999)].

$$(\mathbf{v} \cdot \nabla) \mathbf{v} = \nabla \frac{\mathbf{v}^2}{2} - \mathbf{v} \times (\nabla \times \mathbf{v}) \quad (12)$$

Vorticity ( $\nabla \times \mathbf{v}$ ) is 0, as there is no source of vorticity or any viscosity, so the wave equation simplifies again to equation 13.

$$S(\mathbf{r}, t) = c^2 \frac{\alpha - 1}{2} \nabla^2 \delta^2 + \nabla^2 \frac{\mathbf{v}^2}{2} - \nabla \cdot \left( \frac{\partial \delta}{\partial t} \mathbf{v} \right) \quad (13)$$

The source term allows for the production of audible sound through the demodulation of a higher frequency signal. As the signal is created by the ultrasound driving field (moving through the source at the speed of sound), it is reinforced coherently by earlier audible signals that are travelling with the ultrasound signal. This reinforcement occurs only in the source region, and a directed beam (in the direction of the original signal) is produced.

### 3.4 Method of Solution

The form of  $\delta$  is postulated to take the form shown in equation 14.

$$\delta = \delta_o + \Delta\delta \quad (14)$$

With a driving field  $\delta_o$  and a small perturbation  $\Delta\delta$ . Substituting this into equation 13 and collecting terms of similar order (similar to perturbation theory [Griffiths(1995)]) yields the following equations.

$$\frac{\partial^2 \delta_o}{\partial t^2} - c^2 \nabla^2 \delta_o = 0 \quad (15)$$

$$\frac{\partial^2 (\Delta\delta)}{\partial t^2} - c^2 \nabla^2 (\Delta\delta) = c^2 \frac{\alpha - 1}{2} \nabla^2 \delta_o^2 + \nabla^2 \frac{\mathbf{v}_o^2}{2} - \nabla \cdot \left( \frac{\partial \delta_o}{\partial t} \mathbf{v}_o \right) \quad (16)$$

Where  $\mathbf{v}_o$  is in terms of the variable  $\delta_o$  (see section 3.5). Any solution that satisfies equation 15 (the linear wave equation) can be used in the inhomogeneous term of equation 16. The form that the driving field  $\delta_o$  takes that can produce acoustic lasing is discussed in the section on real emitters (section 5). Once this driving field is chosen, all that remains is to solve for  $\Delta\delta$  (see the section on Green's Functions, section 4).

### 3.5 Form of $\mathbf{v}$

This simplified equation 16 is still in terms of the  $\mathbf{v}$  variable. A relation between  $\mathbf{v}$  and  $\delta$  is found using equation 1 with the Lagrangian formalism (following the fluid particle), rather than the Eulerian formalism (with respect to a fixed origin) used so far [Landau and Lifshitz(2004)]. In the Lagrangian formalism, equation 1 becomes equation 17.

$$\rho_o \frac{d\mathbf{v}}{dt} = -\nabla p \quad (17)$$

Using the equation of state (equation 3) as well as the definition of the fractional change in density (equation 6),  $\mathbf{v}$  can be re-written in the form given in equation 18.

$$\mathbf{v} = \frac{p_o}{\rho_o} \nabla \int (\delta + 1)^\gamma dt \quad (18)$$

It is acceptable to expand equation 18 in a binomial expansion (as  $\delta$  is small) and to only keep *1st order terms*. When the expansion of equation 18 is substituted into 13, any terms higher than first order will produce terms that are higher than 2nd order in  $C$ , which have already been neglected.

## 4 Green's Function for the Scalar Wave Equation

Green's functions are a method of solving inhomogeneous differential equations. While it is often used in electrodynamics to find solutions to Laplace's equation, a Green's function does exist for the wave equation (as it does for any differential equation that can be separated into Sturm-Liouville type [Arfken and Weber(2001)]). The wave equation Green's function is a function that satisfies equation 19.

$$\frac{\partial^2 G}{\partial t^2} - c^2 \nabla^2 G = -4\pi \delta(\mathbf{r} - \mathbf{r}') \delta(t - t') \quad (19)$$

Where  $\delta$  is the Kronecker Delta function in this case, not the fractional change in density. This is the only time that this notation is used.  $G$ , the Green's function, describes the propagation of the signal from a point located at  $\mathbf{r}'$  and  $t'$ . Once  $G$  has been found, it can be used to solve the inhomogeneous wave equation with any boundary condition. A complete description is found in [Morse and Feshback(1953)]. For a signal going to 0 at infinity as well as the function and it's first derivative disappearing at  $t = 0$ , the solution to equation 16 is given by the following integral (equation 20).

$$\Delta \delta = -\frac{1}{16\pi^2} \iiint dV' \frac{S(\mathbf{r}', t - \frac{|\mathbf{r} - \mathbf{r}'|}{c})}{|\mathbf{r} - \mathbf{r}'|} \quad (20)$$

$$S(\mathbf{r}, t) = c^2 \frac{\alpha - 1}{2} \nabla^2 \delta_o^2 + \nabla^2 \frac{\mathbf{V}_o^2}{2} - \nabla \cdot \left( \frac{\partial \delta_o}{\partial t} \mathbf{v}_o \right) \quad (21)$$

## 5 Real Emitters

A discussion of the shape of the intensity distribution of real emitters (speakers) is important for 2 reasons. Firstly, it provides a standard with which the directivity of the acoustic laser can be compared. Secondly, it makes it possible to find the form of  $\delta_o$ .

Monopole emitters are simply point emitters that send out radiation isotropically. The intensity of the signal falls off as  $\frac{1}{distance^2}$ . They are very simple, but they are important, as they are used extensively in the point model (section 6). The Green's function for the wave equation also describes a monopole emitter.

Other types of emitters are dipole emitters and baffled pistons. Dipole emitters are familiar from electromagnetic theory and are used quite often there. In acoustics, they are less prevalent (but they do exist). A more interesting type of emitter is the baffled piston. Most real speakers have an intensity pattern similar to the baffled piston. The approximate intensity pattern from a baffled piston is given in equation 22 ([Hall(1987)]).

$$I = 4I_o \frac{J_1^2(ka \sin \theta)}{k^2 a^2 \sin^2 \theta} \quad (22)$$

Where  $J_1$  is a Cylindrical Bessel Function of the first kind,  $a$  is the radius of the piston, and  $\theta$  is an angle measured from a direction perpendicular to the surface of the piston. The amplitude of the resultant signal is proportional to the square root of equation 22. The intensity distribution is plotted (in polar co-ordinates) in figure 2 for a number of different frequencies (at a piston radius of 0.03 cm).

As  $f$ , the frequency, increases, the directionality of a baffled piston also increases. A reasonable approximation for the shape of this distribution at high frequencies would be a narrow cylinder. The signal passing through this cylinder would be effectively a plane wave as it is confined directly in front of the baffled piston. So at high frequencies, it is reasonable to approximate the radiation pattern from a baffled piston as a plane wave traveling along the axis of a long, narrow cylinder.<sup>4</sup>

## Part III Models

### 6 Point Model

#### 6.1 Timed Speakers and the Green's Function

The Green's function describes how a signal emanating from a point propagates in time and space. The integral in equation 20 is equivalent to turning all of space into a set of point emitters, with their strengths being dictated by the inhomogeneous source term

---

<sup>4</sup>Large arrays of speaker can be used to optimize the shape and strength of the interaction region. This is the idea behind the *parametric acoustic array*.

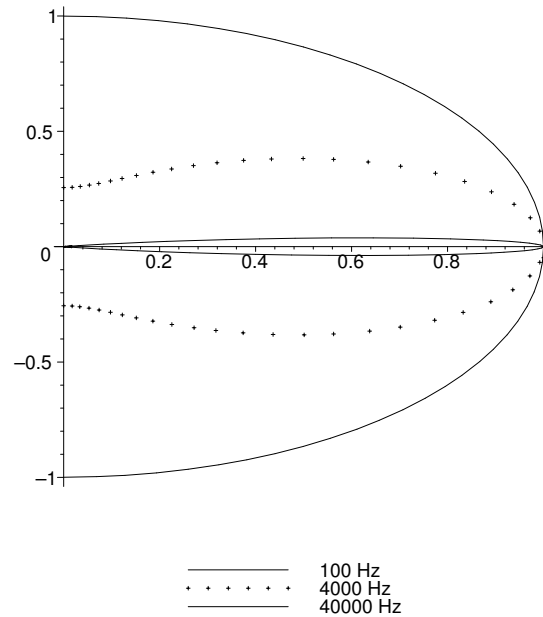


Figure 2: Intensity Pattern from a Baffled Piston for  $f = 0.1, 4, 40KHz$

(equation 21). The  $-\frac{|\mathbf{r}-\mathbf{r}'|}{c}$  in the time dependence creates a set of phase matched point emitters.

This result is used to model the action of an acoustic laser approximately. Rather than performing the integral in equation 20, a discrete set of timed point emitters approximates the integral. This is useful in that it is computationally much less intensive than performing a multi-dimensional integral (Appendix B) and it is physically more intuitive. It also provides a starting point for calculating approximate analytic estimates, as well as comparison with the numerical integration of equation 20.

## 6.2 Line Distribution

The simplest system to model is a number of point emitters in a line. Each emitter emits like a monopole emitter. Physically, this is like placing a number of speakers in a line, and timing them so that they emit when the signal from an adjacent speaker reaches it. This results in the amplitude reinforcing in one direction.

### Analytic Results

The amplitude of a signal from  $N$  emitters placed along the  $\hat{z}$  direction, starting at  $z = 0$ , and each emitter separated by a distance  $a$  is given in equation 23.

$$A(\mathbf{r}, t) = \sum_{n=1}^N \frac{f(|\mathbf{r} - na\hat{z}| - ct + na)}{|\mathbf{r} - na\hat{z}|} T_n(t) \quad (23)$$

$$T_n(t) = 1 - \frac{1}{e^{\frac{(vt-na)}{\alpha}} + 1} \quad (24)$$

Where  $f$  is the signal function (ie. an oscillating function, or a pulse),  $\alpha$  is a small number and  $c$  is the signal propagation speed. The  $T_n(t)$  function acts as a “turn on” function, that allows the emitter to emit only after the signal from previous emitter has reached it. This is important for looking at transient behaviour (like pulses, or oscillating signals at small times). Equation 24 has the form of a Fermi-Dirac distribution for mathematical convenience. A more elegant choice for  $T_n(t)$  would have been a Heaviside step function, but this proved difficult to evaluate in practice.

Each term of the sum in equation 23 corresponds to a different point emitter, located at  $na$  along the  $\hat{z}$  axis. Each point is phased appropriately to constructively interfere along the  $\hat{z}$  direction.

If a sinusoidal signal from the point emitter is used, an approximate form for the angular spreading of the beam can be found. Away from the  $\hat{z}$  axis, the signals from different emitters begin to get out of phase with each other. An approximate angular spread in the far field is given by equation 25.

$$\theta \approx \sqrt{\frac{\lambda}{l}} \quad (25)$$

Where  $\lambda$  is the wavelength of the signal, and  $l$  is the length of the line of emitters. Obviously, the shorter the wavelength or the longer the line, the more directed the beam becomes.

## Numerical Results

All of the numerical work was performed on a 32-bit AMD processor. All programs were written in the C programming language. The signal propagation speed  $c$  was always set to 1 to make the length scales in the problem easier to understand. The line source was implemented in two different ways. The first modeled the action of a number of point emitters in a line, with the timing of the emitters being controlled by a series of control structures. The second involved turning equation 23 into an integral, and evaluating that integral numerically. This was achieved using a recursive trapezoidal rule algorithm ([W.H. Press and Flannery(2002)]) with a fractional accuracy of  $10^{-4}$ . A small number was added to the denominator to prevent divergence, and adjusted so that it did not appreciably affect the final results. Each method provided the same result, and required about the same amount of time.

The results demonstrate a definite directionality in the beam, as shown in figure 3. The results also agreed reasonably well with equation 25 (in this case,  $\lambda = 0.9$  and

$l = 4$ ). Peak height intensity ( $\propto \text{amplitude}^2$ ) was found to drop off as  $\frac{1}{\text{radius}^2}$  outside the source region, as expected. This is shown in figure 4. The length of the source is 4 in the units on the graph and contains 100 point sources in total. In this region, the intensity of the signal increases linearly.

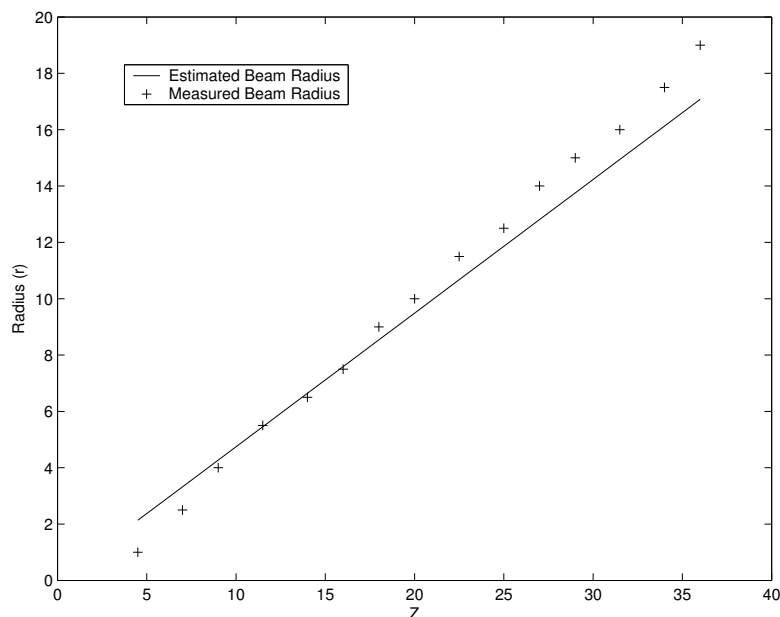


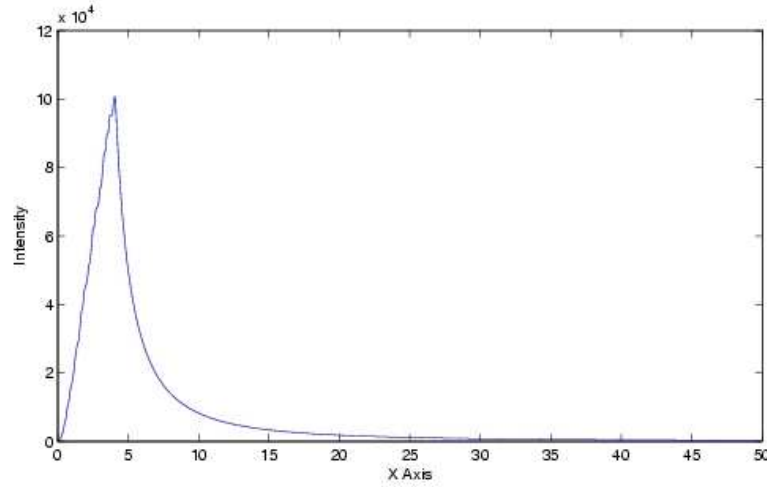
Figure 3: Approximate and Calculated Spread of a Signal From a Line Source

### 6.3 Cylindrical Distribution

For the multi-dimensional integral in equation 20 to be solved, the initial driving field  $\delta_o$  must be determined. A plane wave traveling along the  $\hat{z}$  direction, that only exists inside of a cylinder (with its axis along the  $\hat{z}$  direction, see Appendix C) was chosen because it was the simplest type of signal and geometry that could be used to model the interaction region of a baffled piston (see section 5). This geometry also made it possible to find approximate analytic results. To have something to compare the integral to, the point model was extended to include this cylindrical distribution of emitters.

#### Analytic Results

Approximations of the angular spread of the beam can be found using equation 23. While this equation is only for a line of emitters, it can be extended for a line of circular apertures, as long as one is only concerned with results in the far field. Huygens Principle says that every point in a wavefront can be considered a source of a spherically spreading wave ([Milonni and Eberly(1988)]). This is the origin of diffraction. Hence,

Figure 4: Peak Height Intensity Along  $\hat{z}$  Direction

for a cylindrical source, every term in the sum in equation 23 has the form of a plane wave diffracting through a circular aperture. In the far field for a cylinder with a small radius, Fraunhofer diffraction can be used. Equation 23 becomes equation 26 for a plane wave passing along the axis of a cylindrical source at large times (dropping the  $T_n(t)$  term).

$$A(\mathbf{r}, t) \approx \sum_{n=1}^N \frac{2J_1\left(\frac{2\pi ar}{\lambda(z-na)}\right)}{\left(\frac{2\pi ar}{\lambda(z-na)}\right) |\mathbf{r} - na\hat{z}|} \quad (26)$$

Where  $J_1$  is a cylindrical Bessel function of the 1st kind and  $a$  is the radius of the cylinder. The oscillating part has been removed because its contribution to the angular spread is the same as it was for the line source (equation 25). The strongest directionality in most cases comes from the cylindrical part, so the oscillating part is neglected in this treatment. The sum in equation 26 can be turned into an integral, which can be simplified and solved in the far field by assuming  $z$  becomes very large. This results in an approximate result for angular spread of the signal, shown in equation 27.

$$\tan(\theta) = \frac{3.8\lambda}{2\pi a} \quad (27)$$

The numerical factor 3.8 is the first root of  $J_1$  ([Arfken and Weber(2001)]). This result seems to imply that the directivity of the beam increases as the radius of the

cylinder increases. This is only true as long as  $z \gg \frac{2\pi}{\lambda}a$  ([Milonni and Eberly(1988)]). Otherwise Fraunhofer diffraction breaks down and the result is no longer valid.

### Numerical Results

Rather than use the analytic result in equation 26, which is only valid in the far field, a different approach was taken to model a cylindrical source. Instead of recalculating the signal from every point, the cylinder was broken into a number of lines pointing along the  $\hat{z}$  direction. The signal from one line along the  $\hat{z}$  axis was calculated using the line model (section 6.2). This result was then translated from  $x = 0$  and  $y = 0$  to a new  $x$  and  $y$  position, and summed with the original field. This was repeated until the original line had been duplicated around the  $z$  axis enough times to approximate a cylinder.

The result was a signal that was roughly symmetric around the  $z$  axis (as the number of lines was increased, the symmetry increased), and that demonstrated a directionality that was higher than the previous line result.

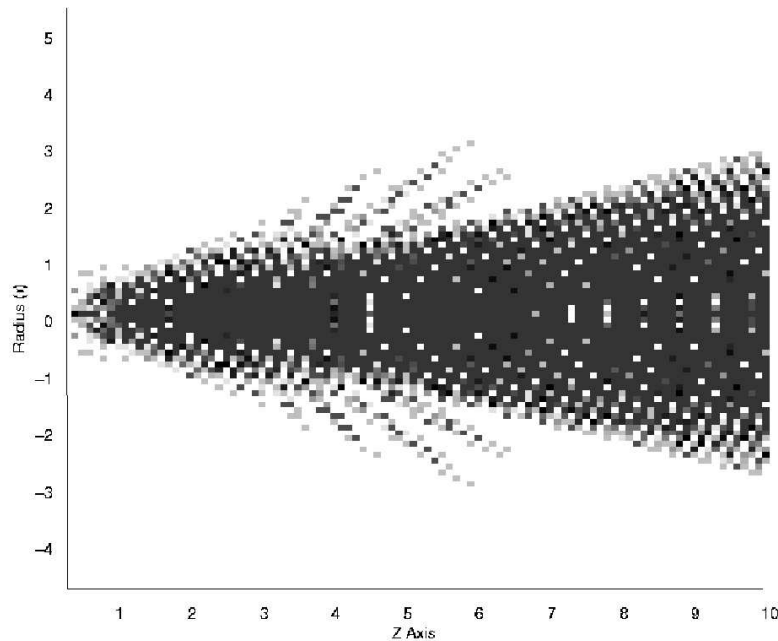


Figure 5: Intensity of Signal from Cylindrical Source

In figure 5, the cylinder radius is 0.5 units and the length is 4 units. This intensity pattern is similar to experimental results obtained in ([Bennet and Blackstock(1975)]). The side lobes in this pattern are also similar to the side lobes that appear in the near field of the baffled piston (equation 22 is only an approximation)([Hall(1987)]).

## 7 Numerical Solutions of the Non-Linear Wave Equations

As was mentioned in section 6.3 a plane wave traveling along the axis of a cylinder was used as the driving field  $\delta_o$ . This provided the simplest geometry that could produce an acoustic laser. A slightly more physical scenario would be a plane wave traveling along the axis of a cylinder with the amplitude of oscillation dropping as  $\frac{1}{z}$  (assuming the cylinder's axis is in the  $\hat{z}$  direction), but not only does this increase the complexity of the source term, it also makes finding approximate analytic results more difficult. It is straight forward to evaluate the source term (equation 21) for an arbitrary signal<sup>5</sup>, but this information would only be really useful in a design problem.

### Gauss-Kronrod Quadrature

Integration of the source term was performed using a Gauss-Kronrod quadrature routine. Gauss-Kronrod quadrature is an extension to regular Gaussian quadrature that makes it possible to evaluate points between the regular nodes of the function you are using (ie. Legendre polynomial, Laguerre polynomials, etc.). They are normally used to estimate the error in the integral using the previously computed points plus the special Kronrod points, rather than going to a higher order polynomial and recomputing all the points ([D. Calvetti and Reichel(2000)]).

As these routines are in general very complicated, an implementation of the QUADPACK libraries for C was used<sup>6</sup>. A 21 point Gauss Kronrod rule was used in a routine that was designed to integrate over “singularities” (sharply peaked points), similar to those found when the integral was evaluated inside the integration cylinder. Divergence was prevented by adding a small term to the denominator. This term was adjusted so that the outside the integration region, the final result was not appreciably affected.

The method that was used to perform the multi-dimensional integral is outlined in Appendix B.

### Analytic Results

The  $\delta_o$  used to evaluate the source term (equation 21) had the following form.

$$\delta_o = C (\cos(k_1 z - \omega_1 t) + \cos(k_2 z - \omega_2 t)) \quad (28)$$

Substituting this into the source term (equation 21), evaluating it in cylindrical polar co-ordinates (see Appendix C) and simplifying with trigonometric identities resulted in a number of terms of different frequencies. These were the original, doubling, sum and difference frequencies, which is what one would expect from a 1st order non-linearity

<sup>5</sup>By this I mean that it is easy to evaluate equation 21 with a computer algebra package for an arbitrary signal. Understanding it is another matter. For a spherically spreading signal from 2 baffled pistons separated from each other by a small distance, be prepared to deal with a 40 page equation.

<sup>6</sup>GNU Scientific Libraries, <http://www.gnu.org/software/gsl>

([Scroggie(1963)]). For an acoustic laser, the term of most interest was the difference term. All other terms were neglected. This was acceptable, as all of the terms were of order  $C^2$  and would not appreciably contribute to further *demodulation*. As well, if driving frequencies in the ultrasound region are used, all of the terms aside from the difference frequencies will be inaudible, and of no interest to an acoustics problem. A result of this simplification is that the driving signal no longer develops into a shock wave.

The final integral for a modulating signal at a single frequency, after much simplification, has the form given in equation 29.

$$\Delta\delta(\mathbf{r}, t) = -\frac{1}{16\pi^2} \int_0^l \int_0^{2\pi} \int_0^a r' dr' d\theta' dz' \frac{1}{|\mathbf{r} - \mathbf{r}'|} \frac{C^2}{\rho_o^2} \left( \frac{p_o^2 \gamma^2}{c^4} (\omega_1 + \omega_2)^2 + \frac{p_o \gamma \rho_o}{c^2} (\omega_1 - \omega_2)^2 \right) \cos \left( (k_1 - k_2) z' - (w_1 - w_2) \left( t - \frac{|\mathbf{r} - \mathbf{r}'|}{c} \right) \right) \quad (29)$$

It is possible to simplify this integral so that an approximate form for the angular spread in the far field can be found. In the far field, expanding  $|\mathbf{r} - \mathbf{r}'|$  and dropping small terms (being careful to not drop terms that are comparable to  $2\pi$  inside the cosine), as well as assuming that the cylinder is very narrow yields an integral that can be performed analytically. The final result is in terms of cylindrical Bessel functions. From this, an approximate form for the angular spread of the beam can be found (equation 30).

$$\tan(\theta) \approx \frac{3.8c}{|\omega_1 - \omega_2|a} \quad (30)$$

This is exactly the same result that was found using the point cylinder model (equation 27)(realizing that  $\frac{c}{\Delta\omega} = \frac{\Delta\lambda}{2\pi}$ ). It is also similar to the first zero of the square root of the intensity distribution for a baffled piston (equation 22)(when  $\theta$  is small). This suggests that the action of an acoustic laser is equivalent to increasing the effective size of a baffled piston (to the radius of the cylinder of ultrasound driving waves, which would normally be larger than the original piston size by equation 22), which in turn increases the directionality of the audible sound.

Using this result, a baffled piston type speaker (radius of 2 cm) with a driving frequency of  $40KHz$  and a modulating frequency of  $1000Hz$  produces intensity pattern that is approximately 40 times more narrow than would be achieved if the  $1000Hz$  signal had been produced directly by the piston.

## Numerical Results

The numerical integration of the source term (equation 29) took considerably longer than the point models, and to a slightly lower degree of accuracy. The final results did

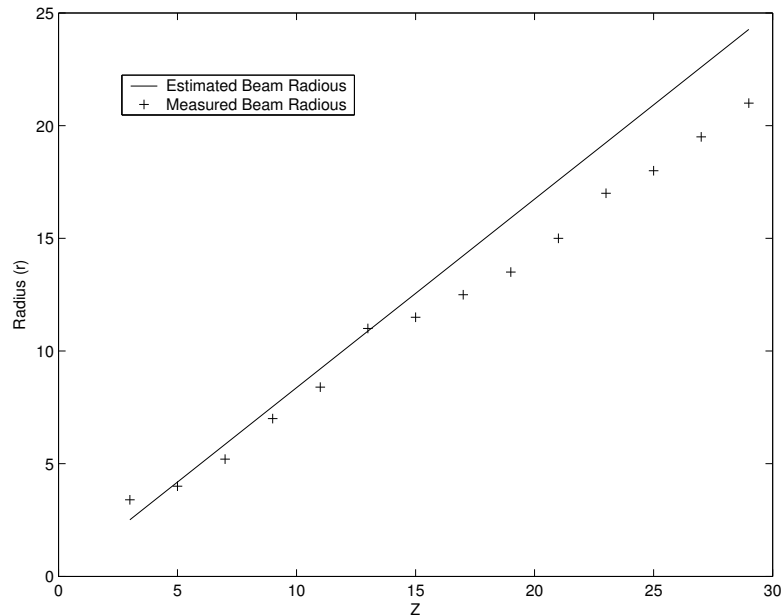


Figure 6: Approximate and Calculated Beam Spreading from a Signal From a Cylindrical Source

yield a directed beam, in agreement with the point cylinder model. The angular spread was in agreement with the approximate result given in equation 30 (figure 6).

In figure 6, the radius of the beam was 0.5 units, and the length 4 units. The wavelength was 1.1.

## Part IV

# Conclusions

The effect of an acoustic laser has been successfully explained and demonstrated. The equations governing this effect have been derived from the fundamental equations of fluid dynamics, and these have been used to numerically model the effect 2 different ways. The results demonstrate an improved signal directionality over conventional baffled pistons. An explanation for this is that the acoustic laser effectively increases the size of the piston, which increases the directionality of the signal.

These methods could easily be extended to more complicated systems and geometries, suitable for an engineering design problem. Fourier techniques could also be used to model more complex signals.

## References

- [Chandani(1998)] S. Chandani, Master's thesis, Queen's University, Department of Physics (1998).
- [Westervelt(1960)] P. Westervelt, *J. Acoust. Soc. Am.* **35**, 535 (1960).
- [Brookner(1985)] E. Brookner, *Scientific American* (1985).
- [Westervelt(1957)] P. Westervelt, *J. Acoust. Soc. Am.* **29**, 199 (1957).
- [Bellin and Beyer(1957)] J. Bellin and R. Beyer, *J. Acoust. Soc. Am.* **32**, 339 (1957).
- [Landau and Lifshitz(2004)] L. Landau and E. Lifshitz, *Fluid Mechanics*, vol. 6 of *Course of Theoretical Physics* (Elsevier Butterworth-Heinemann, 2004), 2nd ed.
- [Blackstock(2000)] D. Blackstock, *Physical Acoustics* (John Wiley and Sons Inc., 2000).
- [Hall(1987)] D. Hall, *Basic Acoustics* (Harper and Row Publishers Inc., 1987).
- [Young and Freedman(1996)] H. Young and R. Freedman, *University Physics* (Addison-Wesley Publishing Company Inc., 1996).
- [Jackson(1999)] J. Jackson, *Classical Electrodynamics* (John Wiley and Sons Inc., 1999), 3rd ed.
- [Griffiths(1995)] D. Griffiths, *Introduction to Quantum Mechanics* (Pearson Prentice Hall Inc., 1995).
- [Arfken and Weber(2001)] G. Arfken and H. Weber, *Mathematical Methods for Physicists* (Harcourt Academic Press, 2001), 5th ed.
- [Morse and Feshback(1953)] Morse and Feshback, *Methods in Theoretical Physics* (McGraw Hill Book Company, 1953).
- [W.H. Press and Flannery(2002)] W. V. W.H. Press, S.A. Teukolsky and B. Flannery, *Numerical Recipes in C* (Cambridge University Press, 2002), 2nd ed.
- [Milonni and Eberly(1988)] P. Milonni and J. Eberly, *Lasers* (John Wiley and Sons, Inc., 1988).
- [Bennet and Blackstock(1975)] M. Bennet and D. Blackstock, *J. Acoust. Soc. Am.* (1975).
- [D. Calvetti and Reichel(2000)] W. G. D. Calvetti, G.H Golub and L. Reichel, *Math. Comput.* (2000).
- [Scroggie(1963)] M. Scroggie, *Second Thoughts on Radio Theory* (Iliffe Books Ltd., 1963).

## Part V

# Appendices

## A Derivation of the Non-Linear Wave Equation

The non-linear wave equation is derived from equations 1 - 3. By equating the gradient of equation 2 with the time derivative of equation 1, one has equation 31.

$$\nabla \cdot \left( \rho \frac{\partial \mathbf{v}}{\partial t} + \rho (\mathbf{v} \cdot \nabla) \mathbf{v} \right) + \nabla^2 p = \frac{\partial^2 \rho}{\partial t^2} + \frac{\partial}{\partial t} \nabla \cdot (\rho \mathbf{v}) \quad (31)$$

The terms  $\nabla \cdot \rho \frac{\partial \mathbf{v}}{\partial t}$  and part of the expansion  $\frac{\partial}{\partial t} \nabla \cdot (\rho \mathbf{v}) = \nabla \cdot \left( \frac{\partial \rho}{\partial t} \mathbf{v} + \rho \frac{\partial \mathbf{v}}{\partial t} \right)$  cancel each other. Using the definition of the fractional change in density ( $\delta = \frac{\rho - \rho_o}{\rho_o}$ ) and subbing it into equation 3 gives equation 32.

$$p = p_o (1 + \delta)^\gamma \quad (32)$$

Equation 32 can be expanded in a binomial expansion to give equation 33.

$$p = p_o \left( 1 + \gamma \delta + \frac{\gamma(\gamma-1)}{2} \delta^2 + \frac{\gamma(\gamma-1)(\gamma-2)}{6} \delta^3 + \dots \right) \quad (33)$$

For small amplitude signals,  $\frac{\partial \mathbf{v}}{\partial t} \gg (\mathbf{v} \cdot \nabla) \mathbf{v}$ , and  $\delta$  is small, so that equation 33 can be truncated after the second term. This leads to equation 5, the linear wave equation.

Substituting equation 33 into equation 31 gives equation 34.

$$\begin{aligned} p_o \nabla^2 \left( \gamma \delta + \frac{\gamma(\gamma-1)}{2} \delta^2 + \frac{\gamma(\gamma-1)(\gamma-2)}{6} \delta^3 + \dots \right) + \\ + \nabla \cdot (\rho (\mathbf{v} \cdot \nabla) \mathbf{v}) = \frac{\partial^2 \rho}{\partial t^2} + \nabla \cdot \left( \left( \frac{\partial \rho}{\partial t} \right) \mathbf{v} \right) \end{aligned} \quad (34)$$

Re-arrangement and substitution of  $\rho = \rho_o \delta + \rho_o$  and  $c^2 = \frac{p_o}{\rho_o} \gamma$  (the signal velocity) into equation 34 gives the following equation (equation 35).

$$\begin{aligned} \frac{\partial^2 \delta}{\partial t^2} - c^2 \nabla^2 \delta = c^2 \frac{\gamma-1}{2} \nabla^2 \delta^2 + \nabla \delta \cdot (\mathbf{v} \cdot \nabla) \mathbf{v} + \\ + (\delta + 1) \nabla \cdot ((\mathbf{v} \cdot \nabla) \mathbf{v}) - \nabla \cdot \left( \frac{\partial \delta}{\partial t} \mathbf{v} \right) - \\ - c^2 \frac{(\gamma-1)(\gamma-2)}{6} \nabla^2 \delta^3 + \dots \end{aligned} \quad (35)$$

All higher order terms come from the binomial expansion of  $p$  (equation 33)(replace the  $(\dots)$  with the term of interest from 33 multiplied by  $\frac{1}{\rho_o}$  and substitute for  $c^2$ ). This is the full non-linear wave equation for a fluid with no viscosity or heat conduction.

## B Multi-Dimensional Integrals

The technique outlined in Section 7 only performs integrals in one dimension. If one wants to extend an integral into higher dimensions, there are two numerical techniques. The first is a Monte-Carlo Simulation. It involves taking random points in your integral space, determining if they lie within the boundaries of your problem, and estimating the integral with the points from your random sample. It is useful if one has a strangely shaped boundary, and a low accuracy is acceptable. Unfortunately, the technique fails when there are strongly peaked regions in the integral, as in the case of the wave equation Green's function.

If one has smooth integration boundaries, a better technique is to break the 3 dimensional integral into three separate one dimensional integrals, in the following way:

$$\begin{aligned}
 I &= \int \int \int dx dy dz f(x, y, z) \\
 g(x, y) &= \int dz f(x, y, z) \\
 I &= \int \int dx dy g(x, y) \\
 h(x) &= \int dy g(x, y) \\
 I &= \int dx h(x)
 \end{aligned}$$

This means that for every  $x$  point,  $y$  must be integrated over. For every  $y$  point,  $z$  must be integrated over. So, if  $n$  function evaluations are needed for a one dimensional integral, the number of function evaluations needed for an  $N$  dimensional integral increases as  $n^N$  [W.H. Press and Flannery(2002)]. Fortunately, computing power has increased to the point where a three dimensional integral is within the abilities of an average personal computer. The advantage of this technique is that a much higher accuracy (compared to a Monte Carlo Simulation requiring a similar number of function evaluations) can be achieved with poorly behaved functions. This technique was used to numerically integrate over equation 29.

Each successive integration must be completed to a higher degree of accuracy than the one before, or the integration routine will not be able to reach its required accuracy. This means that integrals in higher dimensions have a lower accuracy than a one dimensional integral.

## C Cylindrical Co-ordinates